HHS Public Access

Author manuscript

Neuron. Author manuscript; available in PMC 2016 March 04.

Published in final edited form as:

Neuron. 2015 March 4; 85(5): 1117–1131. doi:10.1016/j.neuron.2015.02.007.

Supply-demand mismatch transients in susceptible peri-infarct hot zones explain the origin of spreading injury depolarizations

Daniel von Bornstädt[1,2], **Thijs Houben**[1,3], **Jessica Seidel**[1], **Yi Zheng**[1], **Ergin Dilekoz**[1,4], **Tao Qin**[1], **Nora Sandow**[5,6], **Sreekanth Kura**[7], **Katharina Eikermann-Haerter**[1], **Matthias Endres**[2,6,8,9], **David A. Boas**[7], **Michael A. Moskowitz**[1], **Eng H. Lo**[10], **Jens P. Dreier**[2,6,11], **Johannes Woitzik**[5,6], **Sava Sakadžić**[7], and **Cenk Ayata**[1,12,*]

[1]Neurovascular Research Laboratory, Department of Radiology, Massachusetts General Hospital, Harvard Medical School, 149 13th Street, 6408, Charlestown, MA, USA 02129 [2]Department of Neurology, Charité - Universitätsmedizin Berlin, Charitéplatz 1, 10117 Berlin, Germany [3]Department of Neurology, Leiden University Medical Center, Albinusdreef 2, 2300 RC Leiden, the Netherlands [4]Department of Pharmacology, Gazi University Faculty of Medicine, Besevler Campus, Ankara, Turkey 06560 [5]Department of Neurosurgery, Charité - Universitätsmedizin Augustenburger Platz 1, 13353 Berlin, Berlin, Germany [6]Center for Stroke Research, Charité - Universitätsmedizin Berlin, Charitéplatz 1, 10117Berlin, Germany [7]Optics Division, MHG/MIT/HMS Athinoula A Martinos Center for Biomedical Imaging, Department of Radiology, Massachusetts General Hospital, Harvard Medical School, 149 13th Street, 6408, Charlestown, MA, USA 02129 [8]German Center for Neurodegenerative Diseases (DZNE), partner site, Charité - Universitätsmedizin Berlin, Charitéplatz 1, 10117 [9]German Centre for Cardiovascular Research (DZHK), partner site, Charité - Universitätsmedizin Berlin, Charitéplatz 1, 10117 [10]Neuroprotection Research Laboratory, Department of Radiology, Massachusetts General Hospital, Harvard Medical School, 149 13th Street, 6408, Charlestown, MA, USA 02129 [11]Department of Experimental Neurology, Charité - Universitätsmedizin Berlin, Charitéplatz 1, 10117 Berlin, Germany [12]Stroke Service and Neuroscience Intensive Care Unit, Department of Neurology, Massachusetts General Hospital, Harvard Medical School, 55 Fruit Street, Boston, MA USA 02114

SUMMARY

Peri-infarct depolarizations (PIDs) are seemingly spontaneous spreading depression-like waves that negatively impact tissue outcome in both experimental and human stroke. Factors triggering

*CORRESPONDING AUTHOR: MGH, 149 13th Street, 6408, Charlestown, MA 02129; Phone: (617) 726-8021; Fax: (617) 726-2547; cayata@partners.org.

AUTHOR CONTRIBUTIONS

DvB, TH, JS, YZ, ED, KEH and TQ conducted the experiments, analyzed the data, and helped draft the manuscript; NS, JPD and JW collected and analyzed the clinical data; SS, DAB, ME, MAM and EHL contributed to data interpretation and manuscript preparation; CA conceived and designed the study, analyzed and interpreted the data, and prepared the manuscript.

PIDs are unknown. Here, we show that somatosensory activation of peri-infarct cortex triggers PIDs when the activated cortex is within a critical range of ischemia. We show that the mechanism involves increased oxygen utilization within the activated cortex, worsening the supply-demand mismatch. We support the concept by clinical data showing that mismatch predisposes to PIDs in human stroke as well. Conversely, transient worsening of mismatch by episodic hypoxemia or hypotension also reproducibly triggers PIDs. Therefore, PIDs are triggered upon supply-demand mismatch transients in *metastable peri-infarct hot zones* due to increased demand or reduced supply. Based on the data, we propose that minimizing sensory stimulation and hypoxic or hypotensive transients in stroke and brain injury would reduce PID incidence and their adverse impact on outcome.

INTRODUCTION

Peri-infarct spreading depolarization waves (PIDs) akin to spreading depression frequently occur in ischemic or hemorrhagic stroke and after head trauma in both animal and human brains (Dohmen et al., 2008; Nedergaard and Astrup, 1986; Nedergaard and Hansen, 1993). It is well established that PIDs worsen tissue outcome by increasing metabolic demand and reducing blood flow (mismatch) in already ischemic but viable penumbra at risk for infarction (Dohmen et al., 2008; Dreier, 2011; Dreier et al., 2006; Eikermann-Haerter et al., 2012; Hartings et al., 2009). Each PID wave expands the infarct core into the penumbra in a stepwise fashion (Nakamura et al., 2010; Shin et al., 2006). Clinically, clusters of PIDs have been associated with neurological deterioration in patients (Dreier et al., 2006). Therefore, PIDs may be a therapeutic target in stroke and other brain injury states (Lauritzen et al., 2010; Leng et al., 2011).

Although the electrophysiological characteristics and metabolic and hemodynamic consequences of PIDs have been well described, triggering factors are unknown. Indeed, PIDs spontaneously originate within the ischemic penumbra in ostensibly random fashion. In peri-infarct tissue, transmembrane ionic gradients are preserved, but critically reduced cerebral blood flow (CBF) and oxygenation and mildly elevated extracellular potassium concentrations render the tissue highly susceptible to anoxic depolarization. Such conditions predict *metastable hot zones*, tenuously maintaining their membrane potential at steady state ischemia. To explain the origins of PID occurrence, we hypothesized that any sudden worsening in metabolic supply-demand mismatch may transiently tip the balance towards anoxic depolarization in these hot zones, triggering a PID.

Supply-demand mismatch can be worsened either by decreasing the supply or by increasing the demand for O_2. Functional activation of the cortex is one way to stimulate cortical metabolism and increase O_2 demand. We therefore reasoned that transient cortical activation by tactile somatosensory stimulation might trigger PIDs, and tested this in a pure cortical distal middle cerebral artery occlusion (dMCAO) model in mice. We monitored and detected PIDs in real-time using their characteristic propagation patterns on continuous laser speckle perfusion imaging as a sensitive and specific surrogate (Eikermann-Haerter et al., 2012; Nakamura et al., 2010; Shin et al., 2007; Shin et al., 2006; Strong et al., 2007; Strong et al., 2006; Yuzawa et al., 2012).

RESULTS

Somatosensory stimulation triggers PIDs

Transtemporal dMCAO induced a characteristic perfusion deficit over the dorsolateral cortex (Figure 1a), which partially overlaps with the primary somatosensory cortex (see below). PIDs (circles) were clearly identified as CBF transients propagating across the imaging field (Movies S1–S4). Because of the apparently random occurrence of spontaneous PIDs, a probabilistic approach was required to statistically test the impact of interventions on PID rate (i.e., chance of PID occurrence, incidence). In non-stimulated mice (n=21), PIDs spontaneously erupted at a rate of 1.6±0.3/hour after dMCAO, distributed relatively evenly throughout the recording period without a particular temporal predilection (n=33 PIDs; Figure 1b, green circles). The average spontaneous PID incidence was 12% [8–16%; 95%CI] within any 5-minute period in unstimulated mice (Figure 1d, green bars). In a separate cohort, we applied light tactile stimulation manually for 5 minutes using a cotton tip applicator over four different anatomical parts (Figure S1, tactile stimulation sites, related to Figures 1–5, 7); stimulation was terminated if a PID occurred sooner (Figure 1c, yellow circles). Stimulation of the contralesional forepaw to activate the ischemic hemisphere triggered a PID more than 60% of the time (Figure 1c, red lines; Figure 1d, red bar). This was five-fold higher than the average spontaneous PID occurrence rate in any 5-minute epoch (Figure 1d, dark green bar). Stimulation of the upper forelimb and shoulder area (hereon referred to as ‘shoulder’ in the figures) was equally effective (Figure 1c, orange lines; Figure 1d, orange bar). The average latency between forepaw or shoulder stimulation onset and PID onset was only 2.8±0.3 min (Figure 1c, inset). In contrast, PID occurrence during whisker pad or hindpaw stimulation was much less effective, and did not statistically differ from non-stimulated mice (Figure 1c, blue lines; Figure 1d, blue bars). The PID occurrence rate during ipsilesional stimulation to activate the non-ischemic hemisphere was virtually identical to non-stimulated mice, and thus completely ineffective (Figure 1c, black lines; Figure 1d, black bar). Electrophysiological recordings in a separate cohort directly confirmed that CBF transients detected by laser speckle were indeed associated with extracellular slow potential shifts characteristic of PIDs (Figure S2, electrophysiological confirmation, related to Figures 1–6).

These data showed that tactile somatosensory stimulation during stroke significantly increases the rate of PID occurrence temporally coupled to the stimulus. The data also suggested that PIDs are not triggered simply by a generalized arousal response to light tactile stimulation, because stimulation of the ipsilesional side to activate the non-ischemic hemisphere did not trigger PIDs more than what would be expected from spontaneously occurring PIDs. Indeed, contralesional forepaw and shoulder stimulations were much more effective in triggering PIDs compared with whisker pad or hindpaw stimulations, suggesting that the location of cortical representation is important.

Somatosensory stimulation-induced PIDs show spatial specificity

When we examined the spatial origin and propagation patterns of spontaneous or induced PIDs, we noted two different patterns (Figure 2a). While more than 80% of all spontaneous and forepaw stimulation-induced PIDs originated from outside the imaging field (Movies S1

and S2), shoulder and upper forelimb stimulation gave rise to PIDs that originated from within the imaging field more than 80% of the time (Figure 2b; Movie S3). To better define the spatial relationship of PID origins to primary somatosensory representations, we electrophysiologically mapped cortical somatosensory evoked potentials (SSEPs) upon stimulation of the four body parts referenced to bregma (Figure S1, SSEP mapping, related to Figures 2 and 3). The sites of PID origin during shoulder and upper forelimb stimulation were within the stimulated primary somatosensory cortex (S1) (Figure 2c). In other words, light tactile shoulder and upper forelimb stimulation triggered PIDs within its cortical representation in S1. A spontaneous or forepaw-induced PID seldom originated within the imaging field (Figure 2b). Although we do not know the exact origin of forepaw-induced PIDs (precluded by the optical imaging technique), it is likely to be the secondary somatosensory cortex (S2) located anterolateral to the ischemic cortex outside the imaging field (Ullmann et al., 2013; Woolsey and Van der Loos, 1970).

Among the stimulated body parts, the whisker pad has the largest cortical representation (i.e., barrel cortex). Because whisker stimulation did not trigger PIDs more than the spontaneous occurrence, the size of the cortical representation was not a determining factor. Rather, the location of cortical representation with respect to the perfusion defect appeared to be important. Whisker barrel cortex was clearly within the severely ischemic core, and thus unlikely to be activated by tactile stimulation (Figure 2c). We confirmed this by showing that whisker SSEPs were completely abolished upon dMCAO (Figure S3, whisker, forepaw and shoulder SSEPs before and after dMCAO, related to Figures 2 and 3). Conversely, hindpaw S1 was often outside the perfusion defect and only mildly ischemic, and therefore, less prone to anoxic depolarization upon transient worsening of supply-demand mismatch. To determine whether a critical range of ischemia in activated cortex was required to predispose tissue to somatosensory-evoked PIDs, we measured residual CBF within each S1 representation during respective tactile stimulations. Only shoulder stimulation triggered a PID within its representation in S1. We found that PIDs were triggered from shoulder and upper forelimb S1 when residual CBF within the stimulated cortex was approximately 30% [27–32%; 95%CI] (Figure 2d). Shoulder stimulation failed to trigger a PID when residual CBF was lower or higher than this narrow range, suggesting that hot zones susceptible to PID induction upon tactile stimulation were within a critical range of ischemic severity. Residual CBF within forepaw, whisker and hindpaw S1 were all either below or above this range, explaining why stimulation did not trigger a PID in their respective S1 cortices (Figure 2d).

Changes in perfusion defect dynamically shift the hot zone

We reasoned that if residual CBF defines the hot zones, then we might be able to convert a previously quiet cortical region (i.e., one that did not develop a PID upon stimulation) into a hot zone by artificially bringing the residual CBF in that region to within the critical range (i.e., ~30%). The perfusion defect in focal cerebral ischemia is indeed dynamic, and shows a tight relationship to systemic blood pressure (BP). We, therefore, induced hypotension (~60 mmHg; Table S1) in a separate cohort of mice during dMCAO. Hypotension decreased the residual CBF within the *hindpaw* S1 to the range identified as the hot zone above. Remarkably, tactile stimulation of the hindpaw, which did not trigger any PIDs in

normotensive mice, now triggered a PID nearly 60% of the time in hypotensive mice (Figure 3a,b; Movie S4), and all but one PID originated from within the hindpaw S1 (Figure 3c). The residual CBF within the hindpaw S1 was 31% [26–37%; 95%CI] when a PID originated from the S1 (Figure 3d). In fact, shoulder stimulation no longer triggered a PID in hypotensive mice more than the spontaneous rate, and the few PIDs that coincided with shoulder stimulation did not originate from shoulder S1. This was presumably because the residual CBF within shoulder S1 has dropped below the critical range in most animals (Figure 3d). These data suggest that location of hot zone is indeed determined by residual perfusion, and as such, can be highly dynamic over time.

Increased O_2 extraction precedes the PID onset in stimulated cortex

We next sought to confirm that tactile stimulation increases oxygen extraction to worsen the supply-demand mismatch as a prelude to PID induction. Using multispectral reflectance imaging, we measured cortical oxyhemoglobin (oxyHb) concentrations and hemoglobin oxygen saturation (satHb) within the shoulder S1 hot zones from which PIDs originated during light tactile stimulation. Upon dMCAO, oxyHb concentrations abruptly decreased to 51±3% (±SEM) of pre-ischemic baseline within shoulder and upper forelimb S1. Tactile stimulation of the shoulder further decreased oxyHb and satHb by another 35–40% from the pre-stimulus level prior to triggering a PID within the same region (Figure 4a,b). In contrast, tactile stimulation did not change oxyHb or satHb in other comparably hypoxic penumbral regions of interest that were outside the shoulder S1 and thus not activated (oxyHb 48±6% of pre-ischemic baseline). These data suggest that shoulder stimulation increased O_2 extraction specifically within its cortical representation, and that the additional metabolic burden triggered anoxic depolarization in this critically hypoperfused hot zone. It is important to note that in non-ischemic brain, oxyHb levels increase rather than decrease upon functional activation as a result of hyperemia (Dunn et al., 2005). Therefore, activation-induced decrease in oxyHb reflects already maximally dilated vessels and O_2 extraction, or impaired neurovascular coupling, so that any further increase in O_2 demand could not be matched.

Normobaric hyperoxia prevents somatosensory stimulation-induced PIDs

If somatosensory activation of the cortex increased the O_2 demand in ischemic penumbra, and worsened the supply-demand mismatch to trigger a PID, we reasoned that improving oxygenation within the peri-infarct hot zone should diminish local pO_2 drop during cortical activation and reduce the PIDs triggered by sensory stimulation. We, therefore, induced normobaric hyperoxia (NBO; 100% O_2 inhalation; arterial pO_2 468±39 mmHg), shown previously to significantly increase O_2 delivery to penumbra and rapidly suppress spontaneous PIDs (Shin et al., 2007), and delivered tactile forepaw stimulation as above. Consistent with our hypothesis, NBO nearly abolished forepaw stimulation-induced PIDs (Figure 4c,d).

Cortical neuronal activation is required for somatosensory stimulation to trigger PIDs

To confirm that sensory stimulation-induced PIDs were indeed triggered by local cortical neuronal activation, we topically applied tetrodotoxin (TTX, 1 μM) to the shoulder S1 through a small craniotomy. TTX abolished somatosensory evoked potentials within 15

minutes (Figure 5a,b). In the dMCAO group with saline applied over the craniotomy, shoulder stimulation triggered PIDs 67% of the time, all of which originated from within the shoulder S1 (Figure 5c, d). TTX markedly suppressed shoulder stimulation-induced PIDs to the spontaneous rate observed in non-stimulated mice (17%; Figure 5c,d). Moreover, both PIDs in the TTX group originated laterally, rather than within the shoulder S1, suggesting that these were spontaneous PIDs unrelated to the stimulation, and that TTX did not directly inhibit spontaneous PIDs or their propagation into S1. Since topical TTX application is not a clinically feasible intervention, we also tested whether pharmacological agents in clinical use can suppress somatosensory stimulation-induced PIDs. For this we treated mice systemically with ketamine, a dissociative anesthetic and glutamate receptor antagonist readily available for use in the intensive care unit, and known to suppress spontaneous PIDs in patients with brain injury (Hertle et al., 2012; Sakowitz et al., 2009). Ketamine (120 mg/kg, intraperitoneal, 10 minutes before MCAO) completely prevented PID occurrence during forelimb stimulation (Figure 5c,d). In separate experiments, we also showed that ketamine did not depress somatosensory evoked potentials (not shown) as reported previously (Kayama and Iwama, 1972).

Transient dips in O_2 supply also trigger PIDs at a high rate

Because sensory stimulation-induced PIDs were associated with a significant drop in regional oxyHb within the activated cortex as a prelude to the PID, we hypothesized that other mechanisms that cause transient supply-demand mismatch, such as systemic hypoxia or hypotension, may also trigger PIDs. To test this, we induced brief episodes (5 min or less) of hypoxia by reducing the fraction of oxygen in inspired air. Transient hypoxia was highly effective, triggering PIDs in 63% of all attempts (Figure 6a,b,c). Transient hypotension, induced for 5 min or less by controlled blood withdrawal and reinfusion, was even more effective (75% of all hypotensive episodes; Figure 6b,c). The latency between hypoxia or hypotension onset and PID occurrence was approximately 2 minutes (Figure 6b, insets). Binary logistic regression analysis revealed that the final arterial pO_2 during the hypoxic transient alone was predictive of PID occurrence ($p=0.002$; $R^2=0.86$). A PID occurred 90% of the time if arterial pO_2 dropped below 90 mmHg ($p=0.003$ vs. pO_2>90mmHg). Neither baseline pO_2 nor the magnitude of pO_2 drop showed a significant association with PID occurrence (Figure 6d). A similar analysis also showed that BP either at baseline ($p=0.004$) or during the hypotensive transient could predict PID occurrence ($p<0.001$; $R^2=0.70$). However, only the final BP during the hypotensive transient made a significant contribution to this prediction ($p=0.037$, Wald criterion). Indeed, a PID occurred 90% of the time if mean arterial BP dropped below 70 mmHg ($p<0.001$ vs. BP>70mmHg). Importantly, topical TTX application did not block hypotensive PIDs (n=2 attempts in 2 mice), further confirming that TTX did not directly inhibit PIDs and that hypotensive PIDs did not require cortical neuronal activation. As with somatosensory stimulation, we confirmed the electrophysiological identity of PIDs in a separate cohort during hypotensive transients (Figure S2, electrophysiological confirmation, related to Figures 1–6).

After showing that hypoxic or hypotensive transients could trigger PIDs, we next turned our attention back to the animals without any intervention (i.e., no somatosensory stimulation, or hypoxic or hypotensive transients), and examined whether spontaneous BP fluctuations

could predict the apparently random spontaneous PID occurrence in this cohort. Data showed that systemic BP dropped by approximately 10% during the 2 minutes preceding a spontaneous PID ($p<0.001$; n=33 PIDs; Figure 6e). This was consistent with the 2-minute latency to PID onset during induced hypotension (Figure 6b, insets). These data suggest that spontaneous BP fluctuations can indeed be the trigger for a subset of apparently spontaneous PIDs.

Supply-demand mismatch predisposes to PID occurrence in human stroke

To obtain evidence for supply-demand mismatch as a predisposing factor for PIDs in human brain, we examined the relationship between tissue pO_2 and PID occurrence in 7 stroke patients who have had a craniectomy as part of their clinical management (Figure 6f). Electrocorticogram using implanted intracranial electrodes detected a total of 157 PIDs during a 5-day monitoring period after hemicraniectomy (median 11, range 8–57 PIDs). Tissue pO_2 values were available during 131 PIDs. Continuous monitoring often revealed a reduction in tissue pO_2 shortly before a PID occurrence (Figure 6g). Compared with baseline tissue pO_2 in the absence of a PID (n=162 measurements; see Methods), average tissue pO_2 immediately preceding a PID was significantly lower (31.4±16.3 versus 21.4±6.3 mmHg, P=0.03; Wilcoxon Signed Rank Test, Figure 6h). In contrast, there was no difference between baseline and pre-PID segments in terms of mean arterial pressure (85.2±10.1 versus 87.4±10.1 mmHg) or intracranial pressure (11.0±4.9 versus 15.1±4.6 mmHg). These data suggest that O_2 supply-demand mismatch predisposes to PID occurrence in ischemic human brain as well.

Somatosensory stimulation increases cumulative PID frequency and worsens tissue outcome

Lastly, to test whether increased frequency of PIDs triggered by tactile stimulation indeed worsens the stroke outcome, we examined tissue perfusion and infarct volume. PIDs have previously been shown to worsen tissue perfusion through vasoconstrictive (i.e. inverse) neurovascular coupling, and expand the infarct volume (Dreier et al., 2002; Hossmann, 1996; Kumagai et al., 2011; Shin et al., 2006). Tactile forepaw and shoulder stimulations starting 10 minutes after MCAO onset significantly increased the average cumulative PID frequency (2.6±0.3/hour) compared to spontaneous PIDs in non-stimulated mice (1.6±0.3/hour; p=0.02; Figure 7a). In accordance with the increased PID rate, the area of perfusion defect progressively expanded starting 10 minutes after MCAO in the stimulated cohort and was almost doubled at 60 minutes (Figure 7b,c). Moreover, infarct volumes were significantly larger in the forepaw and shoulder stimulated group 24 hours after 1 hour transient MCAO (Figure 7d); the difference persisted at 72 hours when examined using routine histology (Figure 7e). In contrast, whisker stimulation, which did not increase PID frequency, did not have any effect on infarct volume. These data indicate that the increase in PID occurrence upon tactile stimulation is capable of worsening the tissue outcome in stroke. Interestingly, Luckl et al. previously noted that continuous 2-hour forepaw stimulation during acute focal cerebral ischemia was associated with two-fold higher PID frequencies in rats, but the increase in infarct volume in their study failed to reach statistical significance (Luckl et al., 2010). Nevertheless, their findings show that the phenomenon is not species-dependent.

Conversely, Lay et al. found that mechanical stimulation of a single whisker for 1 second every 20 seconds during the first 2 hours of permanent dMCAO in rats abolished the infarct; however, stimulation was unlikely to trigger PIDs in their study because of its brief duration and single whisker stimulation, and because stimulated S1 was within their infarct core (Lay et al., 2010). In subsequent studies the same group showed similarly improved outcomes after entire whisker pad stimulation irrespective of stimulus durations (Davis et al., 2011). Therefore, our data appeared to contradict their findings. To resolve the discrepancy, we studied an additional cohort after permanent dMCAO and followed their stimulation protocol, but once again did not observe an effect on infarct volume at 24 hours (Figure S5, infarct volumes, related to Figure 7). The sources of this discordance are unclear at this time, but may be species-dependent.

DISCUSSION

Altogether, these data provide compelling evidence for the existence of *metastable hot zones* within the peri-infarct tissue where any further worsening of supply-demand mismatch precipitates anoxic depolarization and triggers a PID with adverse consequences on ischemic tissue outcome (Figure 8). Such hot zones lie within a narrow critical range of hypoperfusion, sufficiently ischemic to render the tissue susceptible, but not ischemic enough to abolish neurotransmission (i.e. electrophysiological penumbra) or to directly precipitate anoxic depolarization (i.e. core). The penumbra is, by definition, electrophysiologically silent, and therefore, susceptible to reduced supply only (i.e. hypoxic or hypotensive transients). The presence and distribution of hot zones are predicted to be highly dynamic and variable both spatially and temporally, based on the artery that is occluded and the fluctuations in the perfusion defect. To add to the complexity, whether a PID is triggered by a given mode of sensory stimulation would depend on the existence of a susceptible hot zone within the activated brain regions, cortical or subcortical. Therefore, the efficacy of specific sensory stimuli in triggering PIDs in our study cannot be extrapolated directly to other stroke models or species.

Nevertheless, the proof-of-principle presented herein probably applies to most if not all strokes caused by large-artery occlusions. This is because rodent dMCAO model yields infarcts that can be considered medium-sized when scaled to human brain. In principle, factors modulating the O_2 supply and demand create spatiotemporally highly dynamic *ripples* of oxygenation in peri-infarct tissue, which are capable of triggering a PID when regional pO_2 dips below the depolarization threshold within a hot zone. Such ripples may be more frequent and larger in magnitude, and cortical somatosensory activation is predicted to be stronger, in awake patients compared with experimental animals kept under steady anesthesia as in our study. Data from the human cohort also provided evidence for worse supply-demand mismatch predisposing to PIDs in stroke patients. It should be noted that although this was a critically ill cohort with large infarcts requiring craniotomies (thereby allowing invasive measurements), the principle applies to milder strokes as well, because in hyperacute stroke there is always a penumbra that is viable but at risk for infarction, and PIDs will harm penumbra regardless of the infarct size. However, considering the extreme variability in the size, location, severity and mechanism of human stroke, as well as the variability in intrinsic tissue susceptibility to ischemic depolarizations (Eikermann-Haerter

et al., 2012), it would be a challenge to predict the type of sensory stimulation that could trigger a PID in any given patient, including tactile, auditory or visual. In this regard, hypoxic and hypotensive transients, which are exceedingly common in stroke patients, are likely to be more potent and predictable PID triggers. Needless to say, the larger the perfusion defect, the larger the perimeter and the hot zone area, the higher the risk of triggering a PID. This principle is well demonstrated in infarcts of various sizes, where small perfusion defects upon distal arterial occlusions generally trigger fewer PIDs compared with larger infarcts upon proximal arterial occlusions (Eikermann-Haerter et al., 2012). The principle also applies to other forms of brain injury, such as subarachnoid hemorrhage, where large artery vasospasm or microvascular dysfunction can create moderately ischemic metastable hot zones from which spreading depolarizations can be triggered during supply-demand mismatch transients.

In light of these findings, certain clinical measures seem prudent to diminish the risk of PID occurrence in stroke patients. For example, simply minimizing somatosensory stimulation in acute stroke, particularly on the side with the deficits, may be a potential precautionary measure in the early stage when PIDs are known to occur most frequently. Clinically available PID inhibitors (e.g., ketamine) should be tested for their efficacy in acute stroke, their sedative effects notwithstanding. Moreover, NBO is highly effective in abruptly suppressing spontaneous as well as somatosensory-induced PID occurrence (Shin et al., 2007). The mechanism appears to involve increased regional O_2 availability in penumbra thereby preventing the ripples of oxygenation from dipping below the depolarization threshold. Along the same lines, higher glucose availability may render hot zones less susceptible to depolarization (Hoffmann et al., 2013) as PID occurrence is inversely related to blood glucose (Nedergaard and Astrup, 1986; Strong et al., 2000). This is an important consideration for the optimal target range for blood glucose in clinical trials of tight euglycemic control in acute stroke. A similar argument can be made for improving collateral perfusion by permissive or induced hypertension (Shin et al., 2008), to reduce the number and size of susceptible hot zones, and to minimize inadvertent hypotensive transients from bringing tissue pO_2 below the depolarization threshold. Therefore, preemptive measures to prevent increased tissue demand, as well as transient hypoxia, hypotension and hypoglycemia could be effective in reducing PID occurrence and their adverse impact on cerebral perfusion and metabolism as well as tissue outcome.

EXPERIMENTAL PROCEDURES

Experimental animals

All experimental procedures were carried out in accordance with the Guide for Care and Use of Laboratory Animals (NIH Publication No. 85-23, 1996), and were approved by the institutional review board (MGH Subcommittee on Research Animal Care, SRAC). Male C57BL6J mice were used in all experiments (6–8 weeks old, 22–28g; Charles River Laboratories).

Systemic physiologic monitoring

All mice were intubated, paralyzed (0.25 mg/ml Rocuronium, Sandoz Canada Inc., Princeton, NJ, USA) and mechanically ventilated (SAR-830 ventilator, CWE Inc. Ardmore, PA, USA), except when tissue outcome was assessed. Arterial pH, pO_2, pCO_2, and blood pressure were measured via a femoral artery catheter (Table S1; PowerLab, ADInstruments, Colorado Springs, MO, USA) under isoflurane anesthesia (2.5% induction, 1.5% maintenance, in 70% N_2O and 30% O_2). Rectal temperature was monitored and maintained at 37°C via a servo-controlled heating pad (FHC, Brunswick, ME, USA).

Distal middle cerebral artery occlusion (dMCAO)

Mice were placed on a stereotaxic frame (Stoelting Co., Wood Dale, IL, USA), scalp reflected via a midline incision, and intact skull overlying the right hemisphere was covered with a thin layer of mineral oil to prevent drying and enhance transparency. A temporal bone burr hole (2 mm diameter) was drilled above the zygomatic arch, and middle cerebral artery was occluded just distal to the inferior cerebral vein using a microvascular clip as described in detail previously (Ayata et al., 2004; Eikermann-Haerter et al., 2012; Shin et al., 2006). Absence of a mechanical CSD induction during drilling was confirmed by laser speckle flowmetry monitoring (see below).

Laser speckle imaging

Cortical perfusion was imaged during dMCAO using laser speckle flowmetry through intact skull. Laser speckle imaging of CBF was performed using a near infrared laser diode (785 nm, 75 mW) and a CCD camera (Cohu 4600, San Diego, CA, USA, 640 × 480 pixels). For laser speckle flowmetry, raw speckle frames were continuously acquired at 2.5 Hz, and multispectral reflectance image frames at the filter wheel rotation frequency of 1.6 Hz.

Multispectral reflectance and laser speckle imaging

Multimodal optical imaging was performed as described in detail previously (Dunn et al., 2003; Dunn et al., 2005). Light for multispectral reflectance imaging was provided by a tungsten halogen fiber-optic bundle (Techniquip R150; Capra Optical, Natick, MA, USA). Before illuminating the sample, light was guided through a filter wheel with six 10-nm-wide bandpass filters (560 to 610 nm) and the diffuse reflectance images were captured by a second CCD camera (Coolsnap fx; Roper Scientific, Tucson, AZ, USA; 1,300 × 1,030 pixels with 3 × 3 binning, resulting in 434 × 343 image size for multispectral reflectance). The illumination light for both imaging modalities was delivered to the sample with an oblique angle, collected by a variable magnification objective (× 0.75 to × 3; Edmund Optics, Barrington, NJ, USA), split by a dichroic mirror, and acquired simultaneously by CCD cameras for combined multispectral and laser speckle imaging. The final multispectral imaging field was positioned over the right hemisphere (~7 × 6 mm^2). The data were subsequently interpolated to the common time base using the recorded filter wheel angular positions and exposure times of both cameras.

Electrophysiological PID recordings during dMCAO

Mice were placed in a stereotaxic frame (David Kopf Instruments, Tujunga, CA, USA) and burr holes were drilled above the right hemisphere under saline cooling at (mm from bregma): (i) posterior 3.5, lateral 2.0 (occipital, 0.5 mm diameter for electrode 1); (ii) anterior 1.0, lateral 2.0 (frontal, 0.5 mm diameter for electrode 2). Dura was kept intact to minimize trauma to the animal. The steady (DC) potential and electrocorticogram were recorded with glass micropipettes (filled with 154 mM NaCl) 300 μm below pia (Axoprobe-1A; Axon Instruments, Buringame, CA, USA). Ag/AgCl reference electrode was placed subcutaneously in the neck. Recording sites were covered with mineral oil after electrode placement to prevent cortical drying. After surgical preparation, cortex was allowed to recover for 15 minutes, and dMCAO was performed during electrophysiological recordings as described above.

Tactile stimulation to trigger PIDs

Mice were manually stimulated with a cotton tipped applicator (size: 15.2 cm; Medline Industries Inc., Mundelein, IL, USA) for a more physiological mode of stimulation, and to allow stimulation of different anatomical regions (contralesional or ipsilesional forepaw, upperforelimb/shoulder, whisker pad and hindpaw) sequentially within the same animal (Figure S1, tactile stimulation sites, related to Figure 1). Stimulation was continued for 5 minutes or until a PID was identified on laser speckle images. In a small subset of animals, stimulation was continued for up to 20 minutes to examine in detail the PID origin; these were not included in statistical comparisons of PID occurrence rates. Ten minutes were allowed after dMCAO onset before the first stimulation, and at least 5 minutes were allowed between each stimulation. Most animals received more than one type of stimulation sequentially in random order. Each stimulus type is shown on a separate panel in Figure 1 for the sake of clarity. Spontaneous PIDs continued to appear between stimulations albeit with lower frequency compared to non-stimulated (i.e., control) mice after dMCAO; these were omitted from the timeline figures again for the sake of clarity. When a spontaneous PID occurred stimulation was delayed for at least 5 minutes. Similarly, at least 5 minutes were allowed after an induced PID before another stimulation was attempted. Entire timelines are shown in Figure S4.

Open cranial window for TTX application on PIDs

For tetrodotoxin (TTX) application onto the S1 cortex, a 1.2 mm diameter burr hole was drilled at 0.5 mm posterior, 2 mm lateral to bregma, under saline cooling, and dura was removed. Inadvertent induction of spreading depression during craniotomy was monitored using laser speckle imaging. 0.05 ml TTX (1 uM) was topically applied onto the cortex for 25 min prior to tactile stimulation to trigger PIDs.

Somatosensory evoked potentials (SSEPs) to demonstrate TTX efficacy

To demonstrate the suppression of cortical evoked activity by topical TTX, animals were anesthetized (isoflurane in 30% O2 and 70% N2) and placed in a stereotaxic frame. An open cranial window was prepared over the right barrel cortex, 1.3 mm posterior and 3.6 mm lateral to bregma. A glass micropipette was placed on the exposed dura and extracellular

SSEPs were recorded relative to an Ag/AgCl reference electrode placed subcutaneously in the neck. Cortical surface was kept moist by 0.9% NaCl solution. Signals were amplified (Axoprobe 1A, Axon Instruments) and digitized for offline analysis (Powerlab/16sp, ADinstruments). Contralateral whisker pad was stimulated in a bipolar fashion by needle electrodes 5 mm apart (700 μA, 150 μs square pulses at 0.1 Hz; A395 stimulus isolator, WPI triggered by an S48 square pulse stimulator, Grass technologies). After locating the maximal SSEP amplitude (~450 μm below dura), baseline SSEPs were recorded for 5 minutes, and TTX (1μM in 0.9% NaCl) was applied topically onto the recording window, and replenished during 30 minutes subsequent recording. SSEPs were averaged offline every 2 minutes and plotted over time.

Electrophysiological mapping of the primary somatosensory cortex (S1)

Under isoflurane anesthesia (70% N_2, 30% O_2), mice were placed in a stereotactic frame. After midline scalp incision to expose the skull, two tungsten electrodes (100 μm tip diameter) were placed on the bone and electrical contact ensured with a drop of electrode gel (signagel, parker laboratories, NJ, USA). One electrode was placed over the hemisphere ipsilateral to the stimulated body side as a reference, and another was used to record SSEPs from S1 contralateral to the stimulated body side. A third electrode was inserted in the tail and used as a ground. Whisker pad, forepaw, shoulder, or hindpaw were stimulated using electrical current pulses (0.1Hz, 150μs, 1 to 3 mA; WPI A390 stimulus isolator) applied through a pair of needle electrodes inserted subcutaneously with an inter-electrode distance of 2–4 mm. A coordinate grid was formed relative to bregma, with a point separation of 500 μm in antero-posterior and medio-lateral axes, relative to bregma (Figure S1). For each body part to be stimulated (in random order in each animal), the recording electrode was placed on the skull at the anticipated coordinate of the center of respective S1 (Franklin, 2008). At least 20 SSEPs were recorded at each coordinate before moving to an adjacent point on the grid. In this way, the size of the recorded area was systematically expanded from the center of S1 along the antero-posterior and medio-lateral axes until SSEP amplitudes dropped to less than 20% of peak, or the edge of the exposed skull was reached. At least 2.5 × 2.5 mm of cortex was mapped for each region. After mapping was complete, the recording electrode was replaced back at the peak SSEP coordinate to confirm stable amplitudes over time; data sets with unstable SSEPs were excluded. The procedure was repeated for each body part. In most animals, 2–3 S1 regions were mapped. The SSEP amplitudes at each coordinate were normalized to maximum amplitude within that region. Peak SSEP coordinates along the antero-posterior and medio-lateral axes were calculated in each animal by Gaussian curve fitting, and then averaged among all animals.

Induction of transient hypoxemia and hypotension

After measuring baseline pH, pCO_2, and pO_2, the fraction of O_2 in the ventilation air was reduced for 5 minutes, or less if a PID occurred sooner. Blood gas measurements were repeated after normoxia was reinstituted. Hypotension was induced by controlled blood withdrawal through the femoral artery catheter for 5 minutes, or less if a PID occurred sooner. Blood pressures at baseline and the end of hypotensive period were noted, and arterial blood was re-infused. At least 5 minutes were allowed between each intervention. Entire timelines are shown in Figure S4.

Induction of stable hypotension to shift the hot zone

Ten minutes after dMCAO, systemic arterial pressure was reduced to ~60 mmHg by controlled blood withdrawal and maintained there throughout the experiment.

Tissue outcome assessments after dMCAO

Spontaneously breathing animals were anesthetized with 1.5 % isoflurane in 70% N_2O and 30% O_2. CBF was monitored by laser speckle imaging. Three cohorts were studied. In the first cohort, 10 min after dMCAO (clip) entire contralesional forepaw and shoulder region was stimulated for 5 min every 5 min to maximally increase PID occurrence rate as described above. In a separate group, whisker pad was stimulated in a similar manner. Control animals did not receive any stimulation after dMCAO. 60 min after dMCAO the clip was removed and successful reperfusion confirmed on laser speckle images. In the second cohort, permanent dMCAO was induced using 10-0 nylon suture ligation. Immediately after dMCAO we applied slow manual whisker stimulation (2 Hz) for 10 minutes, as described previously (Davis et al., 2011). Immediately after stimulation, anesthesia was discontinued and animals transferred to their cages. Once again, control animals did not receive any stimulation after dMCAO. In the first and second cohorts, mice were sacrificed 24 hours after reperfusion. Infarct volume was calculated by integrating the infarct area on 1 mm-thick, 2,3,5-triphenyltetrazolium chloride (TTC)-stained coronal sections. In the third cohort, forepaw and shoulder-stimulated and control (i.e., non-stimulated) mice were sacrificed 72 hours after 1 hour dMCAO and reperfusion, coronal cryosections obtained every 1 mm, and stained with hematoxylin and eosin. Infarct areas were integrated along the anteroposterior axis to calculate the infarct volume.

Human intracranial electrocorticogram and tissue pO_2

The study was approved by the local research ethics committee of the Charité Universitätsmedizin Berlin. Informed consent was obtained from the patient or legal representative. In seven patients (2 female/5 male) with a median age of 60 years (range 44–68 years) and malignant hemispheric stroke, the infarct border was determined by laser speckle contrast imaging (MoorFLPI, Moor Instruments Ltd., Axminster, UK) during decompressive surgery(Woitzik et al., 2013). A probe to measure tissue partial pressure of oxygen ($p_{ti}O_2$) (Licox, Integra LifeSciences, USA) was implanted 10 mm from the infarct in still vital subpial cortex. Next to it, a 6-contact platinum subdural electrocorticography (ECoG) recording strip (Ad-Tech Medical, Racine, WI, USA) was placed over the peri-infarct tissue as depicted in Fig 3. Patients were transferred to the intensive care unit where tissue pO_2, ECoG, mean arterial pressure (MAP) and intracranial pressure (ICP) were continuously recorded during 5 days post-surgery. Mean tissue pO_2 values were determined during a 5 min period prior to each PID. Moreover, mean baseline tissue pO_2 values were determined from 5 min periods taken every two hours unless a PID had occurred two hours before or after. For each patient, the average of the tissue pO_2 values before PID was calculated as well as the average of the baseline tissue pO_2 values. The seven mean values of tissue pO_2 before PID from the seven patients and the corresponding seven baseline tissue pO_2 values were statistically compared.

Data analysis and statistics

Data were presented as fraction of total (%), box-whisker plot (line, median; +, mean; box, 25–75% range; whiskers, min-max) or mean±standard error, and analyzed using χ^2 test, one-way ANOVA followed by Holm-Sidak's or Tukey's multiple comparisons test, two-way ANOVA for repeated measures followed by Sidak's multiple comparisons test, paired or unpaired t-tests, and Wilcoxon signed rank test, where appropriate. The statistical method used to analyze each data set is indicated in respective figure legends.

Supplementary Material

Refer to Web version on PubMed Central for supplementary material.

Acknowledgments

Supported by grants from the NIH (NS055104, NS061505), the AHA (11SDG7600037), the Fondation Leducq, the Heitman Foundation, the Ellison Foundation, the Konrad-Adenauer-Foundation, the Deutsche Forschungsgemeinschaft (DFG-WO 1704/1-1, DFG DR 323/5-1, Excellence cluster NeuroCure; SFB TR 43, KFO 247, KFO 213), EU (European Stroke Network, WakeUp, Counterstroke), Corona Foundation and Bundesministerium für Bildung und Forschung (Center for Stroke Research Berlin, 01 EO 0801).

References

Ayata C, Dunn AK, Gursoy OY, Huang Z, Boas DA, Moskowitz MA. Laser speckle flowmetry for the study of cerebrovascular physiology in normal and ischemic mouse cortex. J Cereb Blood Flow Metab. 2004; 24:744–755. [PubMed: 15241182]

Davis MF, Lay CC, Chen-Bee CH, Frostig RD. Amount but not pattern of protective sensory stimulation alters recovery after permanent middle cerebral artery occlusion. Stroke. 2011; 42:792–798. [PubMed: 21317269]

Dohmen C, Sakowitz OW, Fabricius M, Bosche B, Reithmeier T, Ernestus RI, Brinker G, Dreier JP, Woitzik J, Strong AJ, Graf R. Spreading depolarizations occur in human ischemic stroke with high incidence. Ann Neurol. 2008; 63:720–728. [PubMed: 18496842]

Dreier JP. The role of spreading depression, spreading depolarization and spreading ischemia in neurological disease. Nat Med. 2011; 17:439–447. [PubMed: 21475241]

Dreier, JP.; Windmüller, O.; Petzold, G.; Lindauer, U.; Einhäupl, KM.; Dirnagl, U. Ischemia caused by inverse coupling between neuronal activation and cerebral blood flow in rats. In: Tomita, M.; Kanno, I.; Hamel, E., editors. In Brain activation and CBF control. Amsterdam: Elsevier; 2002. p. 487-492.

Dreier JP, Woitzik J, Fabricius M, Bhatia R, Major S, Drenckhahn C, Lehmann TN, Sarrafzadeh A, Willumsen L, Hartings JA, et al. Delayed ischaemic neurological deficits after subarachnoid haemorrhage are associated with clusters of spreading depolarizations. Brain. 2006; 129:3224–3237. [PubMed: 17067993]

Dunn AK, Devor A, Bolay H, Andermann ML, Moskowitz MA, Dale AM, Boas DA. Simultaneous imaging of total cerebral hemoglobin concentration, oxygenation, and blood flow during functional activation. Opt Lett. 2003; 28:28–30. [PubMed: 12656525]

Dunn AK, Devor A, Dale AM, Boas DA. Spatial extent of oxygen metabolism and hemodynamic changes during functional activation of the rat somatosensory cortex. Neuroimage. 2005; 27:279–290. [PubMed: 15925522]

Eikermann-Haerter K, Lee JH, Yuzawa I, Liu CH, Zhou Z, Shin HK, Zheng Y, Qin T, Kurth T, Waeber C, et al. Migraine mutations increase stroke vulnerability by facilitating ischemic depolarizations. Circulation. 2012; 125:335–345. [PubMed: 22144569]

Franklin, K.; Paxinos, G. The Mouse Brain in Stereotaxic Coordinates. 3. San Diego: Academic Press; 2008.

Hartings JA, Strong AJ, Fabricius M, Manning A, Bhatia R, Dreier JP, Mazzeo AT, Tortella FC, Bullock MR. Spreading depolarizations and late secondary insults after traumatic brain injury. J Neurotrauma. 2009; 26:1857–1866. [PubMed: 19508156]

Hertle DN, Dreier JP, Woitzik J, Hartings JA, Bullock R, Okonkwo DO, Shutter LA, Vidgeon S, Strong AJ, Kowoll C, et al. Effect of analgesics and sedatives on the occurrence of spreading depolarizations accompanying acute brain injury. Brain. 2012

Hoffmann U, Sukhotinsky I, Eikermann-Haerter K, Ayata C. Glucose modulation of spreading depression susceptibility. J Cereb Blood Flow Metab. 2013; 33:191–195. [PubMed: 22968322]

Hossmann KA. Periinfarct depolarizations. Cerebrovasc Brain Metab Rev. 1996; 8:195–208. [PubMed: 8870974]

Kayama Y, Iwama K. The EEG, evoked potentials, and single-unit activity during ketamine anesthesia in cats. Anesthesiology. 1972; 36:316–328. [PubMed: 5020641]

Kumagai T, Walberer M, Nakamura H, Endepols H, Sue M, Vollmar S, Adib S, Mies G, Yoshimine T, Schroeter M, Graf R. Distinct spatiotemporal patterns of spreading depolarizations during early infarct evolution: evidence from real-time imaging. J Cereb Blood Flow Metab. 2011; 31:580–592. [PubMed: 20700132]

Lauritzen M, Dreier JP, Fabricius M, Hartings JA, Graf R, Strong AJ. Clinical relevance of cortical spreading depression in neurological disorders: migraine, malignant stroke, subarachnoid and intracranial hemorrhage, and traumatic brain injury. J Cereb Blood Flow Metab. 2010; 31:17–35. [PubMed: 21045864]

Lay CC, Davis MF, Chen-Bee CH, Frostig RD. Mild sensory stimulation completely protects the adult rodent cortex from ischemic stroke. PLoS ONE. 2010; 5:e11270. [PubMed: 20585659]

Leng LZ, Fink ME, Iadecola C. Spreading depolarization: a possible new culprit in the delayed cerebral ischemia of subarachnoid hemorrhage. Arch Neurol. 2011; 68:31–36. [PubMed: 20837823]

Luckl J, Baker W, Sun ZH, Durduran T, Yodh AG, Greenberg JH. The biological effect of contralateral forepaw stimulation in rat focal cerebral ischemia: a multispectral optical imaging study. Frontiers in neuroenergetics. 2010:2. [PubMed: 20725519]

Nakamura H, Strong AJ, Dohmen C, Sakowitz OW, Vollmar S, Sue M, Kracht L, Hashemi P, Bhatia R, Yoshimine T, et al. Spreading depolarizations cycle around and enlarge focal ischaemic brain lesions. Brain. 2010; 133:1994–2006. [PubMed: 20504874]

Nedergaard M, Astrup J. Infarct rim: effect of hyperglycemia on direct current potential and [14C]2-deoxyglucose phosphorylation. J Cereb Blood Flow Metab. 1986; 6:607–615. [PubMed: 3760045]

Nedergaard M, Hansen AJ. Characterization of cortical depolarizations evoked in focal cerebral ischemia. J Cereb Blood Flow Metab. 1993; 13:568–574. [PubMed: 8314912]

Sakowitz OW, Kiening KL, Krajewski KL, Sarrafzadeh AS, Fabricius M, Strong AJ, Unterberg AW, Dreier JP. Preliminary evidence that ketamine inhibits spreading depolarizations in acute human brain injury. Stroke. 2009; 40:e519–522. [PubMed: 19520992]

Shin HK, Dunn AK, Jones PB, Boas DA, Lo EH, Moskowitz MA, Ayata C. Normobaric hyperoxia improves cerebral blood flow and oxygenation, and inhibits peri-infarct depolarizations in experimental focal ischaemia. Brain. 2007; 130:1631–1642. [PubMed: 17468117]

Shin HK, Dunn AK, Jones PB, Boas DA, Moskowitz MA, Ayata C. Vasoconstrictive neurovascular coupling during focal ischemic depolarizations. J Cereb Blood Flow Metab. 2006; 26:1018–1030. [PubMed: 16340958]

Shin HK, Nishimura M, Jones PB, Ay H, Boas DA, Moskowitz MA, Ayata C. Mild induced hypertension improves blood flow and oxygen metabolism in transient focal cerebral ischemia. Stroke. 2008; 39:1548–1555. [PubMed: 18340095]

Strong AJ, Anderson PJ, Watts HR, Virley DJ, Lloyd A, Irving EA, Nagafuji T, Ninomiya M, Nakamura H, Dunn AK, Graf R. Peri-infarct depolarizations lead to loss of perfusion in ischaemic gyrencephalic cerebral cortex. Brain. 2007; 130:995–1008. [PubMed: 17438018]

Strong AJ, Bezzina EL, Anderson PJ, Boutelle MG, Hopwood SE, Dunn AK. Evaluation of laser speckle flowmetry for imaging cortical perfusion in experimental stroke studies: quantitation of perfusion and detection of peri-infarct depolarisations. J Cereb Blood Flow Metab. 2006; 26:645–653. [PubMed: 16251884]

Strong AJ, Smith SE, Whittington DJ, Meldrum BS, Parsons AA, Krupinski J, Hunter AJ, Patel S, Robertson C. Factors influencing the frequency of fluorescence transients as markers of peri-infarct depolarizations in focal cerebral ischemia. Stroke. 2000; 31:214–222. [PubMed: 10625740]

Ullmann JF, Watson C, Janke AL, Kurniawan ND, Reutens DC. A segmentation protocol and MRI atlas of the C57BL/6J mouse neocortex. Neuroimage. 2013; 78:196–203. [PubMed: 23587687]

Woitzik J, Hecht N, Pinczolits A, Sandow N, Major S, Winkler MK, Weber-Carstens S, Dohmen C, Graf R, Strong AJ, et al. Propagation of cortical spreading depolarization in the human cortex after malignant stroke. Neurology. 2013; 80:1095–1102. [PubMed: 23446683]

Woolsey TA, Van der Loos H. The structural organization of layer IV in the somatosensory region (SI) of mouse cerebral cortex. The description of a cortical field composed of discrete cytoarchitectonic units. Brain Res. 1970; 17:205–242. [PubMed: 4904874]

Yuzawa I, Sakadzic S, Srinivasan VJ, Shin HK, Eikermann-Haerter K, Boas DA, Ayata C. Cortical spreading depression impairs oxygen delivery and metabolism in mice. J Cereb Blood Flow Metab. 2012; 32:376–386. [PubMed: 22008729]

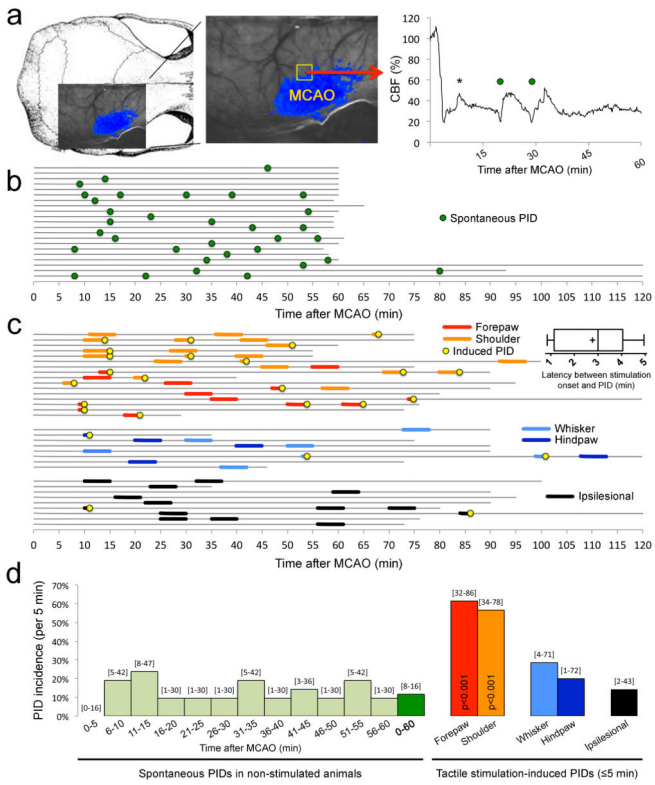

Figure 1. Somatosensory stimulation triggers PIDs in stroke

a. Laser speckle imaging field was positioned over the right hemisphere as shown overlaid on a mouse skull (left panel). Distal middle cerebral artery occlusion (MCAO) induced a focal reduction in cerebral blood flow (CBF) in dorsolateral cortex (middle panel). Blue pixels indicate regions with less than 30% residual CBF after MCAO. We detected PIDs using the propagating large amplitude CBF transients on high spatiotemporal resolution full-field images (Movies S1–S4), as shown in the representative CBF tracing (right panel) from ischemic penumbra (yellow square). Global CBF fluctuations also occurred (*), often linked to systemic transients; these were distinguished from PIDs by lack of propagation on movies.

b. In control (i.e., non-stimulated) animals, PIDs spontaneously occurred in apparently random fashion throughout the MCAO (green circles). Each horizontal line represents one animal, and the start and end of each line indicate the time span of imaging.

c. Light tactile stimulation of the contralesional forepaw and shoulder (red and orange, respectively) triggered a PID within 5 minutes (yellow circles) with high incidence ($p<0.001$ vs. spontaneous PID rate). Inset shows the latency between forepaw or shoulder stimulation onset and PID onset. In contrast, contralesional whisker pad or hindpaw stimulation (light and dark blue, respectively), and ipsilesional stimulation to activate the non-ischemic contralesional hemisphere (black) did not differ from the spontaneous PID rate in non-stimulated mice. Importantly, somatosensory stimulation did not alter systemic blood pressure ($\Delta BP=-1\pm1$ mmHg). Tactile stimulation sites are shown in Figure S1. Electrophysiological confirmation of extracellular slow potential shifts characteristic of

PIDs is shown in Figure S2. Entire timelines from all experiments can be found in Figure S4.

d. Because tactile stimulation was delivered for 5 minutes, we quantified the spontaneous PID occurrence rate in non-stimulated mice as average PID incidence within each 5-minute period (i.e., the chance that a PID will occur within any 5-minute period). Spontaneous PIDs occurred throughout the MCAO at an average 5-minute incidence of 12% (dark green) without a strong temporal predilection (light green). Contralesional forepaw or shoulder stimulation dramatically increased PID incidence during the 5-minute stimulation period ($p<0.001$ vs. spontaneous PID rate; χ^2 test). In contrast, contralesional whisker pad or hindpaw stimulations, or ipsilesional stimulation (7 forepaw, 4 shoulder, 3 hindpaw), did not differ from the spontaneous PID rate in non-stimulated mice. 95% confidence intervals are indicated above the bars.

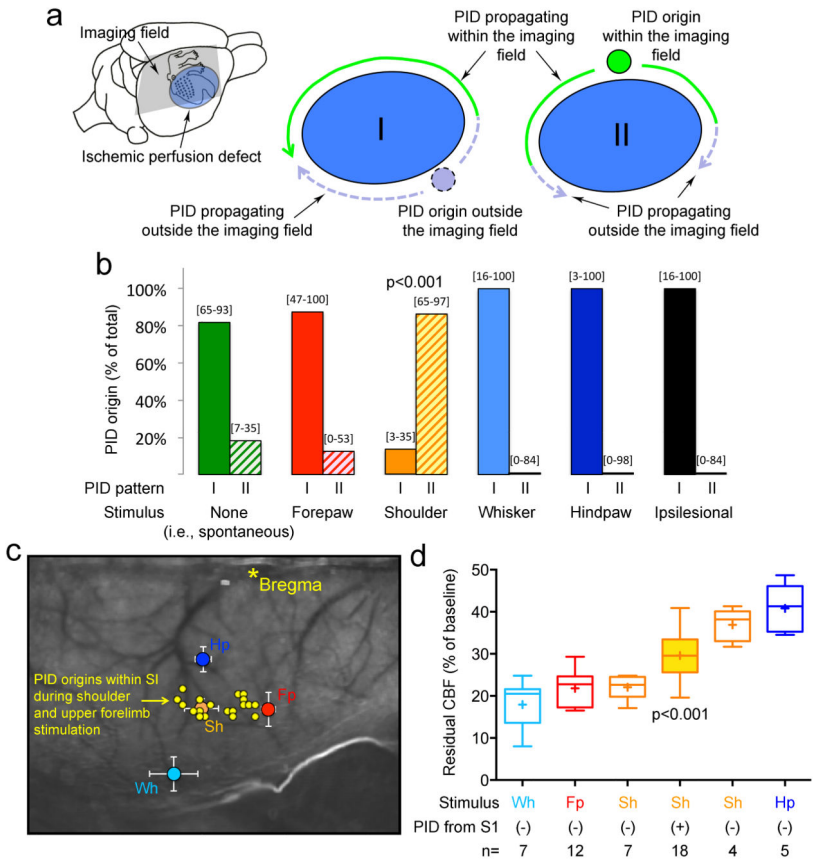

Figure 2. Somatosensory stimulation triggers PIDs within an activated hot zone at a narrow critical range of ischemia

a. The location of the perfusion defect (blue) after MCAO in relation to the primary somatosensory cortex (S1), and PID origin and propagation patterns. Because of the dorsal cortical position of the imaging field (gray shaded area), lateral boundary of the perfusion defect and temporal cortex were poorly visualized. PIDs originated either outside the imaging field (pattern I) or within (pattern II). PIDs originating outside the imaging field often emerged anteriorly and propagated along the medial border of the perfusion defect (pattern I; Movie S1); the mirror wave propagating posteriorly along the lateral border likely collided with and was annihilated by the wave propagating along the medial border, and therefore, it was often not directly visualized (dashed lines; see Movie S2). PIDs that originated within the imaging field (pattern II) usually did so within the S1 cortex and propagated centrifugally (solid green lines; Movies S3 and S4).

b. Spontaneous PIDs, and PIDs that coincided with forepaw, whisker, hindpaw or ipsilesional stimulation predominantly originated outside the imaging field (pattern I), while shoulder (and upper forelimb) stimulation gave rise to PIDs almost exclusively from a medial focus (pattern II; $p<0.001$; χ^2 test).

c. Laser speckle contrast image showing the locations of primary (S1) forepaw (Fp, red), shoulder (Sh, orange), whisker (Wh, light blue) and hindpaw (Hp, dark blue) sensory cortices mapped using evoked potentials (referenced to bregma; see Figure S1 for details). Shoulder and upper forearm stimulation-induced PIDs (yellow circles) that originated within

the imaging field (n=15) did so exclusively within their S1 representations (shoulder, see Figure S1, orange outlined region). In 9 additional attempts, shoulder stimulation was continued for up to 20 minutes until a PID occurred. In 5 of these, a PID occurred (56%), 4 of which also originated from within the stimulated S1. Hence, altogether a total of 19 PIDs originated within the shoulder and upper forearm S1 during shoulder and upper forearm stimulation.

d. Residual CBF values within the stimulated whisker (Wh), forepaw (Fp), shoulder (Sh) and hindpaw (Hp) S1 cortex are shown as a measure of ischemic severity at the onset of stimulation. Only shoulder and upper forearm stimulation triggered PIDs within its S1. We divided the shoulder stimulation attempts based on whether a PID was triggered within the activated S1 (filled bar) or not (empty bars). We further subdivided the latter into 2 groups based on residual CBF above or below the mean residual CBF in the PID (+) group. PIDs were triggered only when residual CBF in activated S1 was within a narrow range ($p<0.001$ vs. all other groups; one-way ANOVA followed by Holm-Sidak's multiple comparisons test). Surface artifacts precluded CBF quantification in one shoulder and one forepaw attempt.

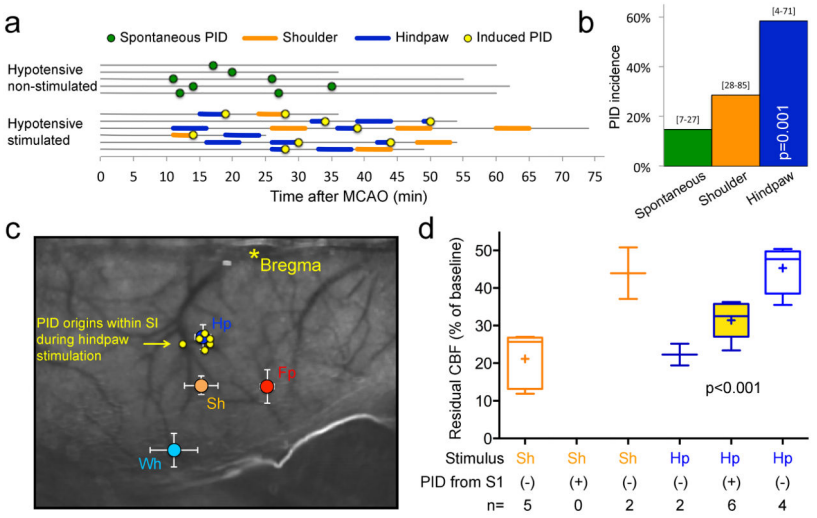

Figure 3. Systemic hypotension dynamically shifts the hot zone within which tactile stimulation triggers PIDs

a. In hypotensive mice that did not receive tactile stimulation (i.e., controls), the spontaneous PID rate after dMCAO did not differ from the normotensive group shown in Figure 1. In contrast to normotensive mice, however, light tactile stimulation of the contralesional hindpaw (dark blue) triggered PIDs within 5 minutes (yellow circles) with high incidence, while shoulder and upper forelimb stimulation (orange) did not consistently trigger a PID over the spontaneous rate.

b. PID occurrence rates (i.e., the chance that a PID will occur within a 5-minute period) are shown in non-stimulated (i.e., spontaneous PIDs) and stimulated mice after dMCAO. Spontaneous PIDs occurred throughout the dMCAO at a rate of 15% (dark green). Contralesional hindpaw stimulation significantly increased PID incidence during the 5-minute stimulation period ($p=0.001$ vs. spontaneous PID rate; χ^2 test). 95% confidence intervals are also shown.

c. All but one hindpaw stimulation-induced PIDs originated from the hindpaw S1, shown superimposed on the S1 map (see Figures 2 and S1 for details).

d. Residual CBF values within the stimulated shoulder (Sh) and hindpaw (Hp) S1 cortex are shown as a measure of ischemic severity at the onset of stimulation. We divided the shoulder stimulation attempts based on whether a PID was triggered within the activated S1 (filled bar) or not (empty bars). We further subdivided the latter into 2 groups based on residual CBF above or below the mean residual CBF in the PID (+) group. PIDs were triggered only when residual CBF in activated S1 was within a narrow range ($p<0.001$ vs. all other Hp groups; one-way ANOVA followed by Holm-Sidak's multiple comparisons test).

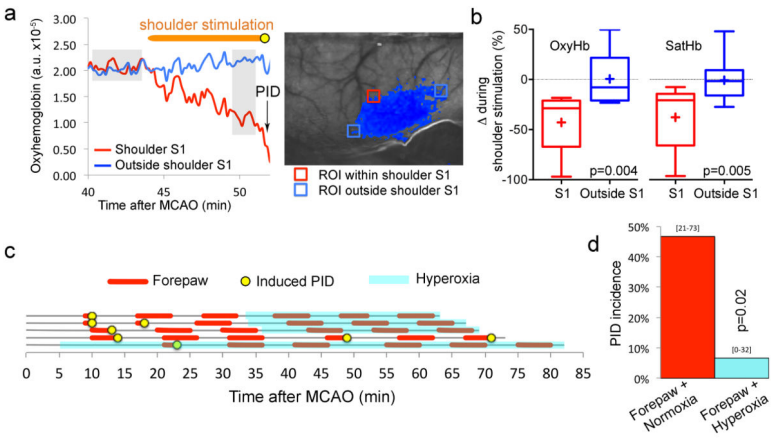

Figure 4. Somatosensory stimulation triggers PIDs by worsening the supply-demand mismatch in activated cortex

a. Representative tracings obtained by multispectral reflectance imaging show that tactile stimulation of the shoulder area (horizontal orange bar) decreases oxyHb concentration within the stimulated S1 (red) but not outside (blue). A PID originated within the activated S1 (arrow, yellow circle). Grey shades indicate the approximate time segments (pre-stimulation baseline and pre-PID, respectively) averaged to calculate the oxygenation changes (ΔoxyHb and ΔsatHb) shown in Figure 4b.

b. Average oxyHb and satHb changes during tactile stimulation of the shoulder area are shown as box-whisker plots (line, median; +, mean; box, 25–75% range; whiskers, min-max range) from within the stimulated S1 (red) and from comparably hypoxic penumbra outside the stimulated S1 (blue). Tactile shoulder stimulation decreased oxyHb and satHb by approximately 35–40% in activated S1, whereas no net change occurred in penumbra outside this region ($p<0.01$; paired t-test).

c. Light tactile stimulation of the contralesional forepaw (red lines) for 5 minutes often induced a PID during the stimulation (yellow circles). In 3 experiments, we instituted normobaric hyperoxia (light blue shade) during the second half of the experiment and repeated the forepaw stimulation. In 1 experiment each, we either did not institute hyperoxia (time control) or instituted it during the entire experiment. Importantly, in this experimental cohort, normoxic ventilation was carried out with 70%N_2/30%O_2 mixture; hyperoxia was instituted by switching the gas mixture to 100% O_2. By doing this, we avoided the confounding effects of changes in N_2O concentrations when switching from normoxia to NBO, and showed that stimulation-induced PID triggering was not influenced by N_2O in other cohorts.

d. Contralesional forepaw stimulation triggered a PID half of the time under normoxic conditions. Hyperoxia markedly reduced the PID occurrence rate during forepaw stimulation ($p<0.05$; χ^2 test). 95% confidence intervals are indicated above the bars.

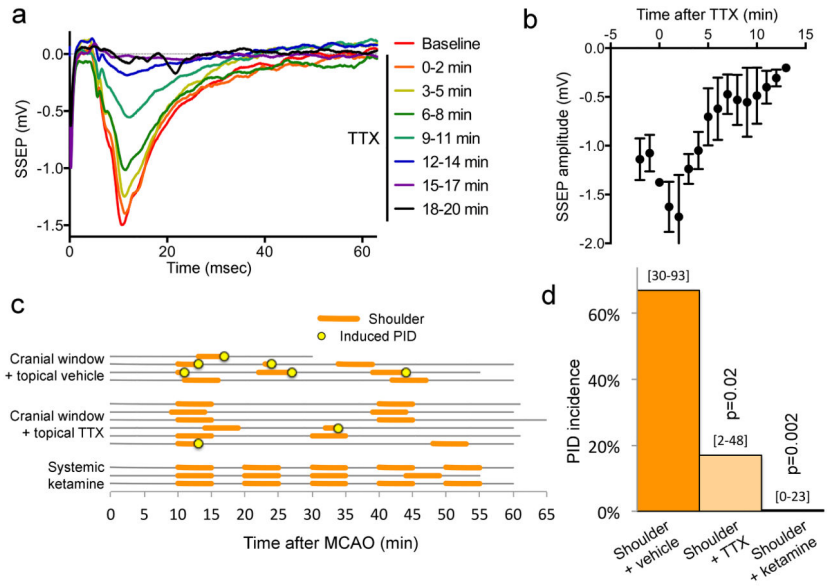

Figure 5. Topical tetrodotoxin (TTX) application diminishes functional activation of the cortex and prevents shoulder stimulation-induced PIDs

a. Somatosensory evoked potentials (SSEPs) were recorded using glass micropipettes from barrel cortex during electrical stimulation of whisker pad in a separate group of normal (i.e. non-ischemic) mice to confirm the efficacy of selected concentration of TTX (1 μM) to suppress SSEPs. Topical application of TTX progressively abolished whisker barrel SSEPs within 15 minutes, as shown in this representative experiment. Average SSEP tracings from successive 2-minute periods are shown in different colors. Barrel cortex was chosen because of its large size.

b. Average SSEP amplitude is shown as a function of time after topical TTX application (n=5).

c. Light tactile stimulation of the contralesional shoulder for 5 minutes (orange lines) induced a PID at a high rate during the stimulation (yellow circles) in the presence of a small cranial window and topical vehicle application (n=4 mice). Topical TTX application markedly diminished PID induction rate during shoulder stimulation (n=6 mice). The two PIDs that occurred during shoulder stimulation under TTX originated outside the shoulder S1, and thus were most likely spontaneous. Systemic ketamine (120 mg/kg, intraperitoneal, 10 minutes prior to stimulation) treatment completely prevented PID occurrence during shoulder stimulation (n=3 mice). Isoflurane concentration was reduced to 0.3 % after ketamine administration.

d. Contralesional shoulder stimulation triggered a PID nearly 80% of the time in the presence of an open cranial window over shoulder S1 and topical vehicle application. Topical TTX markedly reduced and systemic ketamine completely prevented PID occurrence during shoulder stimulation ($p<0.05$; χ^2 test). 95% confidence intervals are indicated above the bars.

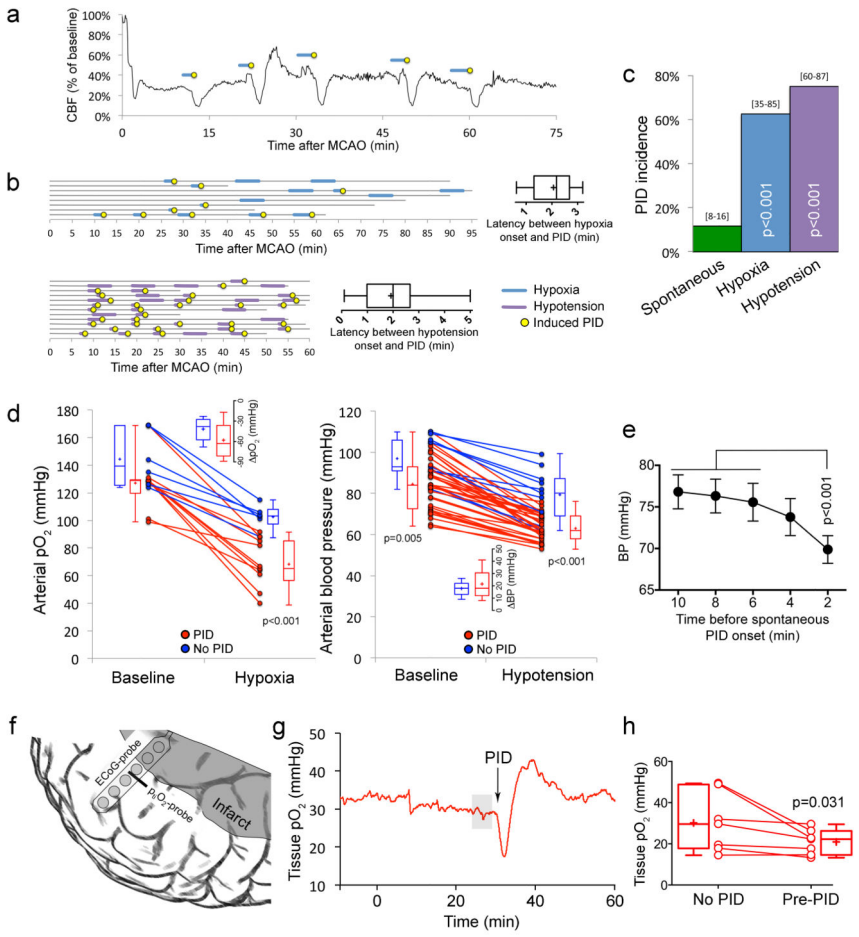

Figure 6. Hypoxic and hypotensive transients consistently trigger PIDs

a. Representative CBF tracing showing 5 PIDs (yellow circles) triggered by transient hypoxic episodes induced by reducing the fraction of O_2 in ventilation gas mixture (blue lines). No spontaneous PID occurred in this experiment.

b. Summary timeline of transient hypoxia (blue lines) and hypotension (purple lines) experiments. Each horizontal line represents one animal, and the start and end of each line indicate the time span of imaging for up to 95 minutes. Insets show the latency between hypoxia or hypotension onset and PID onset.

c. Hypoxia (blue bar) or hypotension (purple bar) triggered PIDs at a markedly higher rate than spontaneous occurrence (green bar, data from control experiments in Figure 1d shown here for comparison; $p<0.05$; χ^2 test). 95% confidence intervals are indicated above the bars.

d. Summary of arterial pO_2 and BP at baseline and during hypoxia (left) or hypotension (right), dichotomized based on whether a PID occurred (red) or not (blue) during each attempt. Individual experiments and averages at baseline and during hypoxic or hypotensive trial are shown for each group. The arterial pO_2 level dropped to a significantly lower level during hypoxia in the group that developed a PID compared to the group that did not. In contrast, neither baseline pO_2 nor the magnitude of pO_2 drop differed between the groups. In hypotension attempts, both baseline and hypotensive BP levels differed between the PID and no PID groups; however, once again final BP alone could predict PID occurrence. Prediction

success was 87.5% (90% for occurrence of a PID and 83.3% for absence of a PID) for final pO_2, and 89.4% (94.4% for occurrence of a PID and 72.7% for absence of a PID) for final BP. A binary logistic regression analysis was conducted to predict the onset of a PID using baseline pO_2, hypoxic pO_2, the magnitude of pO_2 drop, baseline BP, hypotensive BP, and the magnitude of BP drop, as predictors.

e. The time course of resting BP during 10 minutes preceding spontaneous PIDs (n=32; BP could not be measured reliably during 1 spontaneous PID). There was on average a 10% drop in resting BP 2 minutes before the occurrence of a spontaneous PID. One-way ANOVA for repeated measures.

f. Depiction of tissue pO_2 probe (ptiO2) and 6-contact platinum subdural ECoG recording strip implanted over peri-infarct tissue guided by laser speckle imaging (see Methods).

g. Representative tissue pO_2 tracing showing the transient dip in O_2 availability preceding a PID in human cortex. Grey shade indicates the 5-minute segment averaged to calculate the pre-PID oxygenation shown in Figure 6h. Baseline levels were selected when there was no PID occurrence within a 2 hour period (see Methods).

h. Mean tissue pO_2 levels prior to PID were significantly lower compared with baseline levels (Wilcoxon Signed Rank Test).

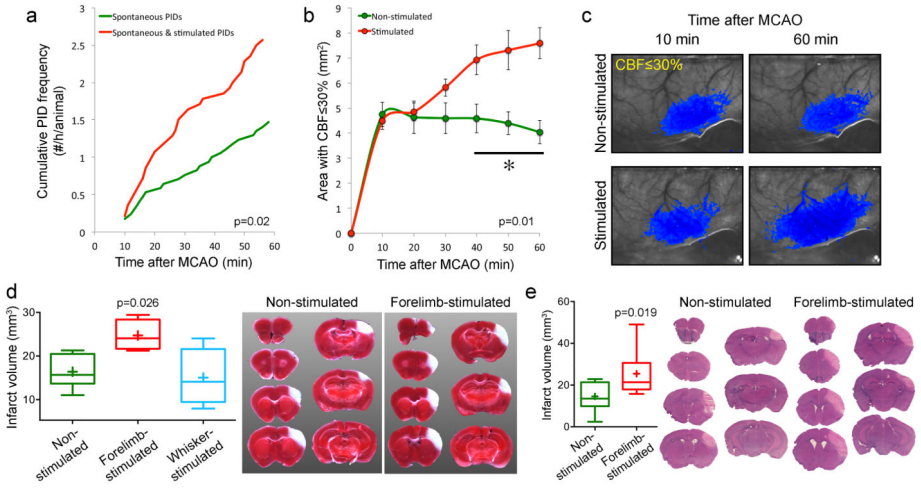

Figure 7. Tactile stimulation-induced PIDs worsen ischemic tissue perfusion and outcome

a. Average cumulative induced and spontaneous PID frequency in mice receiving tactile stimulation starting 10 minutes after MCAO (red, n=14), and spontaneous PID frequency in non-stimulated controls (green, n=17). None of the mice in these cohorts were subjected to transient hypoxia or hypotension as part of the experimental protocol.

b. Area of perfusion defect with ≤30% residual CBF increased in proportion with PID occurrence in the stimulated group over time. Two-way ANOVA for repeated measures.

c. Representative laser speckle flowmetry images showing the expansion of perfusion defect (blue pixels with ≤30% residual CBF) between 10 and 60 minutes after MCAO in a mouse that received tactile stimulation, and the stable perfusion defect in a mouse without tactile stimulation.

d. Infarct volumes measured using TTC staining were larger in the group receiving forepaw but not whisker stimulation starting 10 minutes after MCAO (n=6, 4 and 4 in control, forepaw and whisker stimulation groups; $p<0.05$; t-test). These experiments were performed in a separate cohort of mice without endotracheal intubation or mechanical ventilation in order to minimize surgical morbidity and mortality. The experimental protocol was otherwise identical to other tactile stimulation experiments above. There were a total of 2.25±0.25 PIDs in the forepaw-stimulated group, whereas no spontaneous or induced PID was detected in non-stimulated and whisker stimulated cohorts, respectively.

e. Infarct volumes measured 72 hours after stroke onset using H&E-stained coronal brain sections were larger in the group receiving forepaw stimulation starting 10 minutes after dMCAO (n=9 each; t-test). In this cohort, we initially studied n=5 mice per group. The data showed higher than expected coefficient of variation. We then performed a power analysis, determined n=10 mice per group as the appropriate sample size, and added 5 more mice in each group. One mouse was excluded in each group based on a priori criteria (1 in non-stimulated group due to total absence of an infarct; 1 in stimulated group due to clip-related trauma precluding reliable infarct measurement). Therefore, final sample sizes were n=9 per group. As with the 24-hour assessment group above, these experiments were performed in a separate cohort of mice without endotracheal intubation or mechanical ventilation in order to minimize surgical morbidity and mortality. In this experimental cohort, inhalation gas included 70%N_2/30%O_2 mixture. By doing this, we also reproduced the effect of

stimulation-induced PIDs on tissue outcome in the absence of N_2O. The experimental protocol was otherwise identical to other tactile stimulation experiments above. Representative sections show the infarct at each slice level in one non-stimulated and forepaw and shoulder stimulated mouse each.

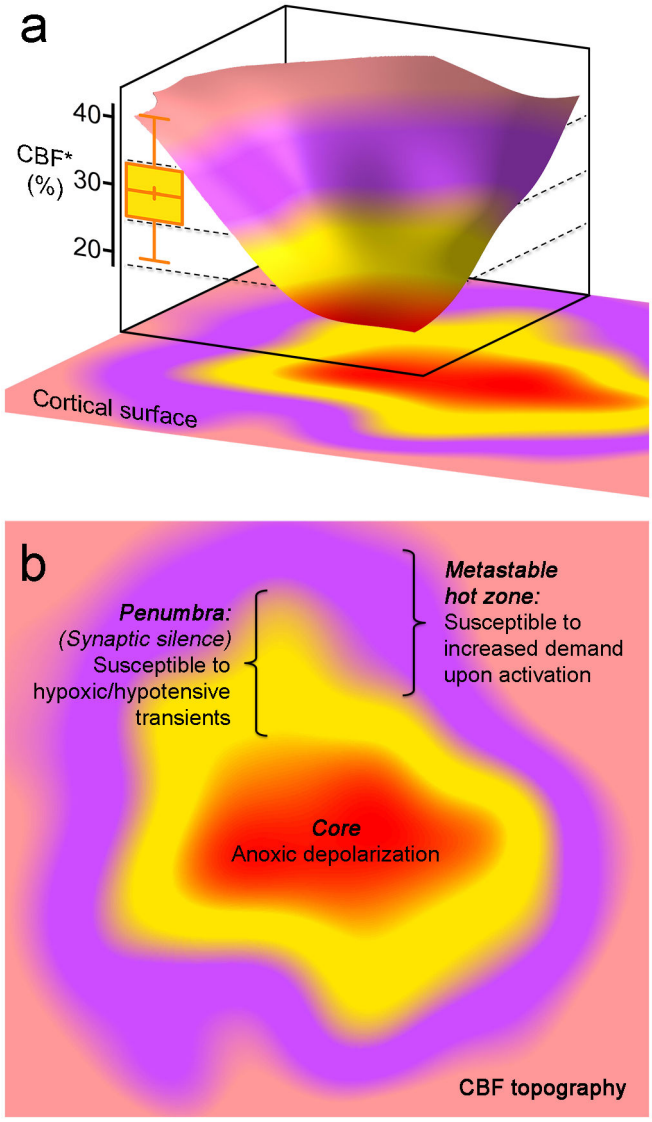

Figure 8. The concept of peri-infarct hot zones susceptible to PID initiation

a. Three-dimensional rendering of a hypothetical CBF defect upon focal arterial occlusion, depicting the conceptual framework consisting of the severely ischemic depolarized core (red), the penumbra (yellow), and the metastable hot zone surrounding it (lavender). The narrow critical CBF range defining the hot zone is also shown from Figure 2d (yellow bar, residual CBF in shoulder S1 where a PID is triggered upon shoulder stimulation).

b. Two-dimensional projection of the perfusion defect. In the metastable hot zone, increased demand during functional activation of the tissue worsens the supply-demand mismatch to trigger a PID. Because penumbra is electrophysiologically silent, by definition it cannot be activated upon somatosensory stimulation; therefore, it is only susceptible to reduced O_2 supply during hypoxic and hypotensive transients to trigger a PID.